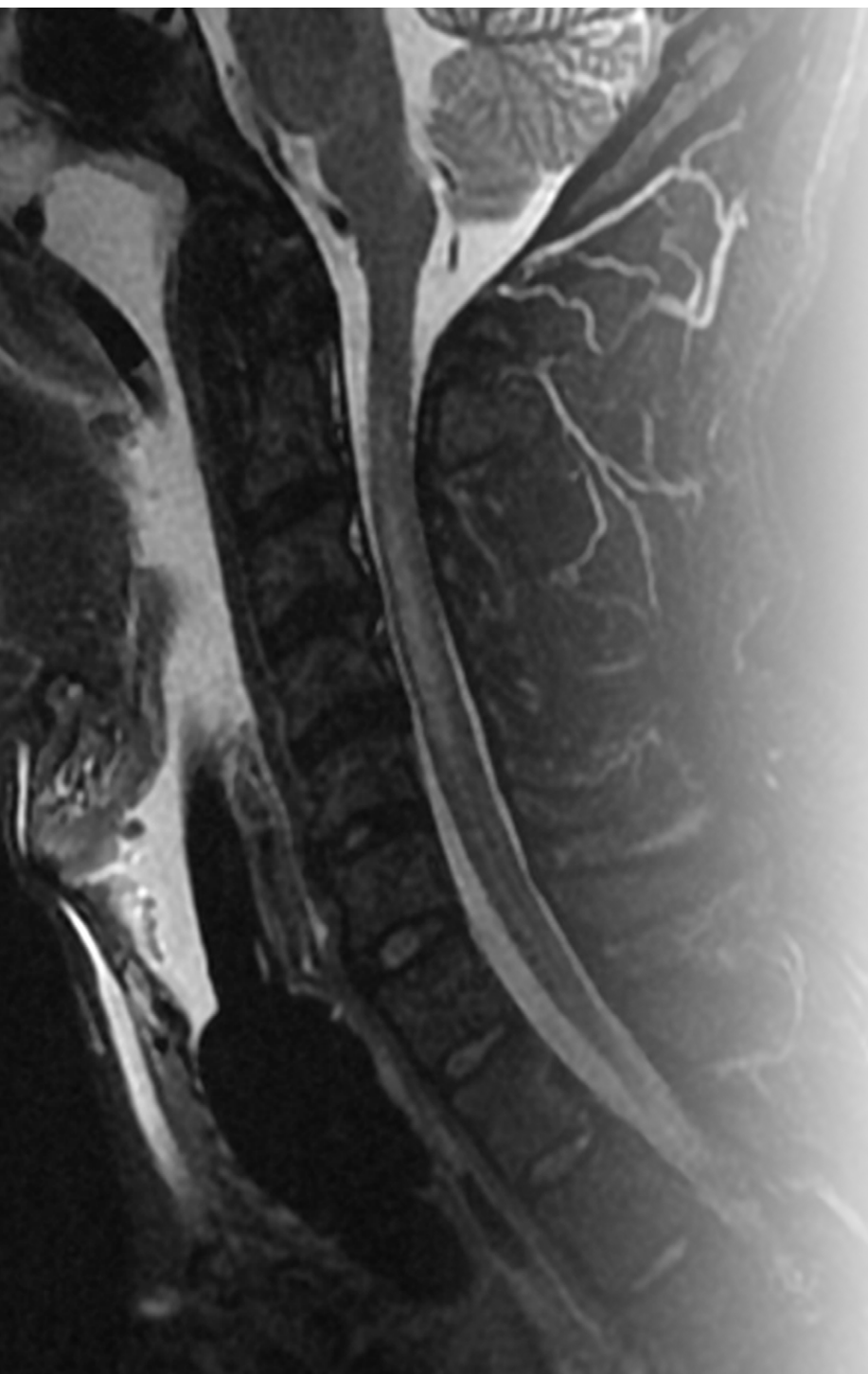


# Vascular Pathologic Conditions in and around the Spinal Cord

Jennifer McCarty, MD • Charlotte Chung, MD, PhD • Rohan Samant, MD • Clark Sitton, MD • Eliana Bonfante, MD • Peng Roc Chen, MD  
Eytan Raz, MD, PhD • Maksim Shapiro, MD • Roy Riascos, MD • Jose Gavito-Higuera, MD

Author affiliations, funding, and conflicts of interest are listed at [the end of this article](#).



Diagnosing and differentiating spinal vascular pathologic conditions is challenging. Small structures, lengthy imaging examinations, and overlapping imaging features increase the difficulty. Yet, subtle findings and helpful protocols can narrow the differential diagnosis. The authors aim to help radiologists make accurate and timely diagnoses of spinal vascular pathologic conditions in and around the spinal cord by highlighting spinal vascular anatomy, imaging findings, and three broad categories of abnormalities: infarcts, anomalies, and tumors.

©RSNA, 2024 • [radiographics.rsna.org](#)

## Introduction

Vascular pathologic conditions in and around the spinal cord can be a diagnostic dilemma with high morbidity. While radiologists are familiar with similar pathologic entities in and around the brain, the small size of the spinal cord and spinal vessels, duration of image acquisition, and range of causes with intrinsic abnormal intramedullary signal intensity present additional challenges (1–3). This can result in misdiagnosis or delayed diagnosis (4–6). A clear understanding of spinal vascular anatomy, optimized spine protocols, and imaging findings of spinal vascular pathologic conditions will help radiologists interpret imaging examinations and guide management.

Spinal vascular pathologic conditions include spinal infarcts, anomalies, and tumors (7). As with those in the brain, ischemic infarcts in the spinal cord are the result of arterial occlusion that has abrupt onset and cytotoxic edema. Spinal vascular anomalies follow the International Society for the Study of Vascular Anomalies (ISSVA) classification with malformations further divided into shunting or nonshunting categories (8). Shunting malformations have many different classification systems and clinical manifestations, but the most important differentiating factors are location (intradural,

**Test Your Knowledge**

**RadioGraphics 2024; 44(9):e240055**  
<https://doi.org/10.1148/rg.240055>

**Content Codes:** CT, MR, NR, VA

**Abbreviations:** ASA = anterior spinal artery, AVF = arteriovenous fistula, AVM = arteriovenous malformation, CVF = cerebrospinal fluid venous fistula, DSA = digital subtraction angiography, DWI = diffusion-weighted imaging, ISSVA = International Society for the Study of Vascular Anomalies, MRA = MR angiography, PSA = posterior spinal artery, SCCM = spinal cord cavernous malformation, TR = time resolved

**TEACHING POINTS**

- The utility of postcontrast TR-MRA of the spine cannot be overstated. TR-MRA can be particularly helpful for confirmation and localization of spinal vascular shunts, raising suspicion for shunting vascular lesions and guiding the angiographers to the correct levels resulting in drastic decreases in contrast media, radiation, and time in the angiography suite.
- The abrupt onset of symptoms and hyperacute course of cord infarcts can help differentiate spinal cord infarcts from other causes of acute intrinsic abnormal T2 spinal cord signal intensity, which include demyelinating, inflammatory, infectious, and idiopathic causes. Symptoms from spinal cord infarcts rapidly progress after onset and usually peak around 12 hours.
- Shunting spinal vascular malformations are defined by their locations (intradural, dural, or epidural) and the presence of a nidus (AVM) or absence of a nidus (AVF). While knowledge of classification systems for AVMs and AVFs is beneficial, the most important thing for diagnostic radiologists to do is raise suspicion of shunting malformations, provide detailed descriptions of imaging findings, and recommend appropriate next steps.
- Venous malformations are the most common type of slow-flow non-shunting simple vascular malformations. They are known by many names. Pathologic conditions termed *cavernous malformation*, *cavernoma*, *cavernous hemangioma*, *epidural hemangioma*, and *intraosseous hemangioma* are all actually slow-flow venous malformations.
- While not true vascular tumors, some neoplastic masses in and around the spinal cord can be hypervascular and have associated shunting. These include but are not limited to hemangioblastoma, solitary fibrous tumors, paragangliomas, and metastases.

dural, extradural) and the presence or absence of a nidus (8,9). Spinal tumors can be true vascular tumors per ISSVA classifications or hypervascular masses, some which develop associated shunting.

**Vascular Anatomy****Arterial Anatomy**

The average adult spinal cord is 1 cm in diameter, 45 cm long, and weighs 35 g (about 2%–3% of the brain) (1). The supplying arteries are similarly small and mostly less than 1 mm in diameter. In contrast, the intracranial arteries such as the M1 middle cerebral artery range from 2 to 5 mm (10,11). The spinal cord is predominantly supplied longitudinally by the anterior spinal artery (ASA) and paired posterior spinal arteries (PSAs) (Fig 1) (12). The ASA is 0.2–0.8 mm in diameter and supplies the anterior two-thirds of the spinal cord. Its territory includes the corticospinal tracts responsible for motor function and the spinothalamic tracts responsible for pain and temperature

sensation. The paired PSAs are smaller at 0.1–0.4 mm in diameter each and combine to supply the posterior one-third of the spinal cord (13). Their territory includes the dorsal columns responsible for proprioception and vibration sensation. Vasocorona arteries traverse between the ASA and PSAs, giving rise to tiny perforator arteries along the surface of the cord (7).

The ASA and PSAs are supplied by an array of axially and obliquely oriented small variable feeding arteries. Embryologically, transverse segmental arteries on both sides at every spinal level supply the spinal cord. As longitudinal connections develop (future ASA, PSAs, and vertebral arteries), most transverse segmental arteries regress, becoming purely radicular and leaving only seven or eight sporadically located radiculomedullary arteries along the length of the spinal cord (12). Technically, purely radicular arteries supply only the nerve root, radiculomedullary arteries supply the nerve root and the spinal cord, radiculopial arteries supply the posterior spinal system, and radiculomedullopial arteries supply all (12). The largest radiculomedullary artery is the radiculomedullary magna artery, also known as the artery of Adamkiewicz (0.8–1.3 mm) (14). It has a characteristic hairpin turn and most often arises between the T8 and L2 vertebrae on the left, although this location can vary (7). The segmental branches of the aorta supply most of the thoracic and lumbar spine. The cervical spinal cord supply receives feeding vessels from the vertebral arteries, subclavian branches (costocervical trunk, thyrocervical trunk, etc), and supreme intercostal artery. The median sacral artery off the aortoiliac bifurcation and the lateral sacral arteries off the iliac arteries contribute to the sacral spine supply (12).

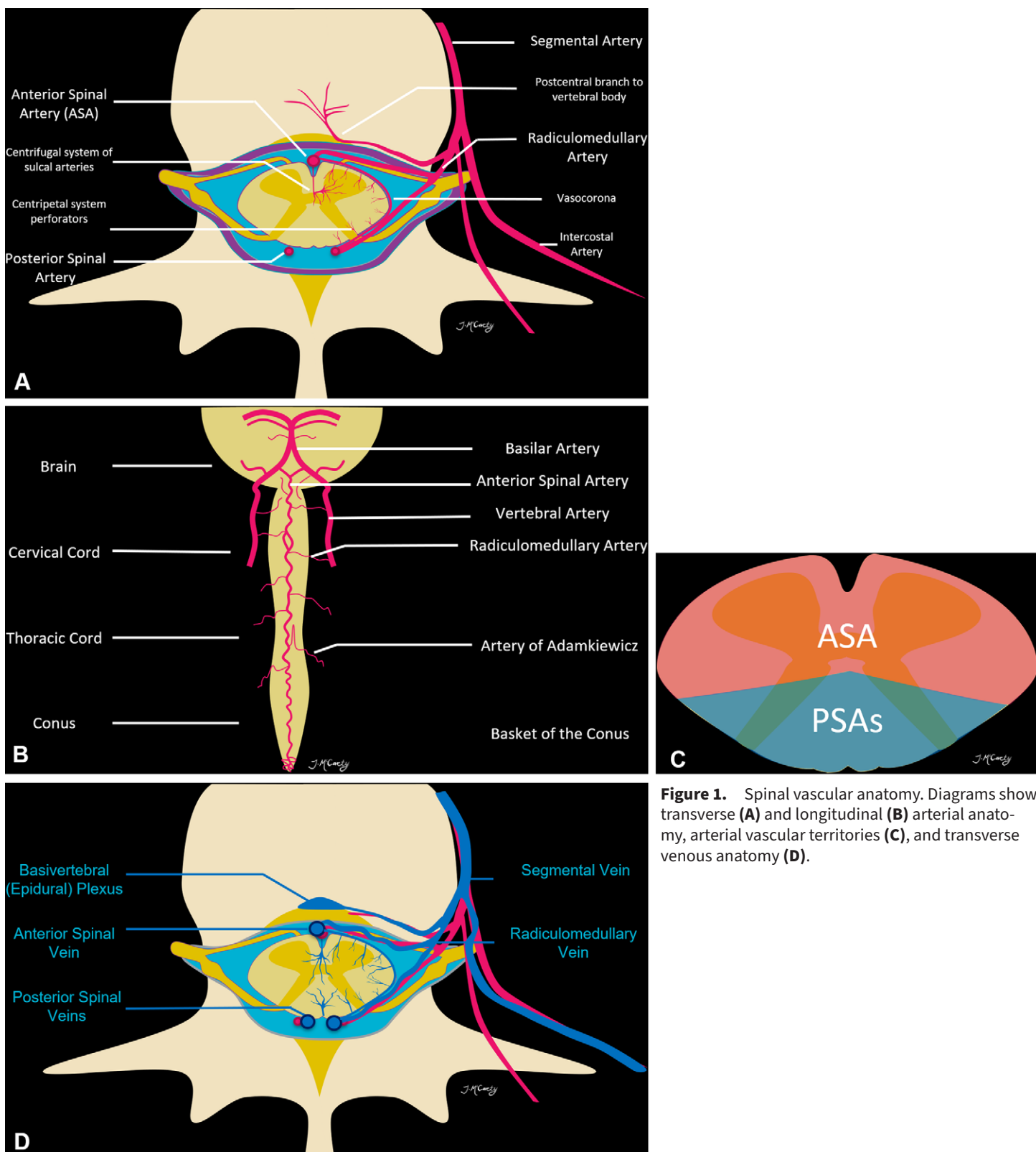
Additional extradural arteries of importance include the ventral and dorsal epidural arcades and the postcentral branches to the posterior one-third of the vertebral body. Longitudinal anastomotic networks continue outside of the spinal canal and are paravertebral, prevertebral, and along the spinous processes (12).

**Venous Anatomy**

A single anterior and two paired posterior spinal veins follow the course of their corresponding arteries. An intradural perimedullary venous plexus traverses around the spinal cord and nerve roots and connects to epidural venous plexi via bridging veins and radiculomedullary veins. The basivertebral vein of the vertebral body drains to the epidural venous plexus in the midline. Each spinal level has a segmental vein on each side. These segmental veins can drain longitudinally into the lumbar veins, azygos vein, and/or inferior vena cava (12).

**Imaging****CT and CT Angiography**

CT and CT angiography may be the workhorses for intracranial pathologic conditions but have traditionally had more limited applications for spinal vascular pathologic conditions. Routine CT is most helpful to exclude osseous compressive causes of myelopathy and delineate pathologic conditions of the tissues around the thecal sac. Currently, CT angiography is most helpful to evaluate larger more proximal vessels,



such as the vertebral arteries and aorta. Improvement in techniques and postprocessing appear promising for better detection and localization of vascular pathologic conditions. Some studies have shown improved characterization of spinal arteries, including the ASA, with a higher contrast media dose (2.0 mL/kg vs 1.5 mL/kg), higher concentration (370

or 400 mg/mL), and slight bolus delay (15,16). Others have shown superior identification of the artery of Adamkiewicz with reduced radiation to 70 kV at CT angiography compared with 120 kV, identifying the artery in 87% of cases (17). Some suggest improved sensitivity and accuracy of spinal vascular malformations with postprocessing techniques for spinal CT

**Table 1: Imaging Modalities for Spinal Vascular Pathologic Conditions**

Modality	Advantages	Disadvantages
CTA	Fast; widely available; osseous evaluation	Radiation; iodinated contrast media; lower sensitivity
MRI	Cord evaluation; flow voids; exclusion of other pathologic conditions; no radiation	Lengthy imaging times; motion degraded; artifacts (especially with DWI); safety screening
MRA	Confirmation and localization of vascular shunts	Gadolinium contrast media; technologist and reader dependent; lower spatial and temporal resolution than those of DSA
DSA	High spatial and temporal resolution; diagnostic with therapeutic options	Invasive; radiation; iodinated contrast media; lengthy examination time; operator dependent

Note.—CTA = CT angiography.

angiography that include multiplanar reformations, bone subtraction, and bone background fusion images (16).

### MR and MR Angiography

MRI and MR angiography (MRA) are the go-to imaging studies for noninvasive spinal vascular pathologic diagnoses. Conventional MRI sequences can help detect spinal cord edema, hemorrhage, enlarged vessels, and tumors. The biggest challenge with MRI of the entire spine is the lengthy examination time given the long craniocaudal extent of the spinal cord and canal. Spinal MRI protocols vary. Traditional protocols can take up to 90 minutes but include T2-weighted imaging, which is helpful for assessing the spinal cord and pathologically enlarged flow voids. Some institutions have implemented emergent focused abbreviated survey techniques (FAST) protocols of the spine for screening, which are then followed by anatomically focused dedicated traditional MRI protocols when abnormalities are detected (2). New MRI deep learning-based MRI reconstructions maintain excellent image quality but speed up the examination, with a reported 70% reduction in turbo spin-echo sequence acquisition time (18).

In addition to standard MRI sequences, diffusion-weighted imaging (DWI) and volumetric (three-dimensional) high-resolution fluid sensitive or heavily T2-weighted imaging (Cube, SPACE, VISTA, CISS, FIESTA, three-dimensional T2-weighted, etc) can be of use in patients with spinal vascular pathologic conditions. Compared with brain DWI, spine DWI *b* values are lower, typically 600 or 800 sec/mm<sup>2</sup>. The sagittal plane is preferred, allowing for an internal comparison (normal cord vs abnormal cord) at a single section. Three-dimensional imaging of the spine can allow exquisite detail of anatomy and pathologic features, and the isotropic sequences allow high-resolution reformations in any plane. Volumetric high-resolution heavily T2-weighted MRI of the spine can be particularly helpful for identification and localization of abnormal flow voids, helping guide the angiographers and surgeons by elucidating dorsal versus ventral abnormalities and identifying the most involving spinal levels (19). These can be acquired in the sagittal plane (in either two or three segments to cover the entire spine) at acquisition times of 6 minutes per segment and subsequently reformatted in coronal and axial planes.

The utility of postcontrast time-resolved (TR)-MRA of the spine cannot be overstated. TR-MRA can be particularly

helpful for confirmation and localization of spinal vascular shunts, raising suspicion for shunting vascular lesions and guiding the angiographers to the correct levels resulting in drastic decreases in contrast media, radiation, and time in the angiography suite (20,21). The field of view is most often from the mid thoracic to mid lumbar spine to include the most common locations of spinal vascular shunts but can differ depending on suspected location. The details depend on the vendor. Protocols have been described with TR imaging of contrast kinetics (TRICKS) where, in less than a minute of total imaging time, more than 25 contrast phases with more than 10 sections each can be obtained with a temporal resolution of 1.8 seconds between acquired phases (20). With a temporal resolution of less than 2 seconds and a bolus of 20 mL of gadolinium contrast media injected at 3 mL/sec followed by a saline bolus, the majority of spinal vascular malformations (>80%) can be localized within one vertebral level. Combining the evaluation of TR-MRA with volumetric high-resolution heavily T2-weighted imaging increases sensitivity and accuracy of spinal vascular malformation diagnosis, classification, and feeder characterization (19).

The quality of the TR-MRA acquisition and interpretation is highly dependent on technologist and reader experience. It can be advantageous to groups to perform postcontrast TR-MRA with certain controls, including restricted hours of acquisition (8 AM through 5 PM, when more help is available), a limited number of magnets, a select group of technologists, and a select group of readers. Importance should be placed on high temporal resolution and early timing as to not miss the arterial phase of the contrast media bolus.

### Catheter Angiography

Digital subtraction angiography (DSA) remains the reference standard for diagnosing spinal vascular pathologic conditions. Its main advantages over other imaging modalities are its superior temporal and spatial resolution (Table 1), but DSA is invasive and quite time intensive. To perform complete spinal catheter angiography, the interventionalist must select and inject each segmental artery on each side at each spinal level. That is why the time savings from selected injections at suspected levels based on TR-MRA findings are highly valued. Additional limitations of DSA include high contrast media doses (200–600 mL), limited ability to acquire true lateral imaging (due to arm and shoulder positioning), and difficulty selecting small

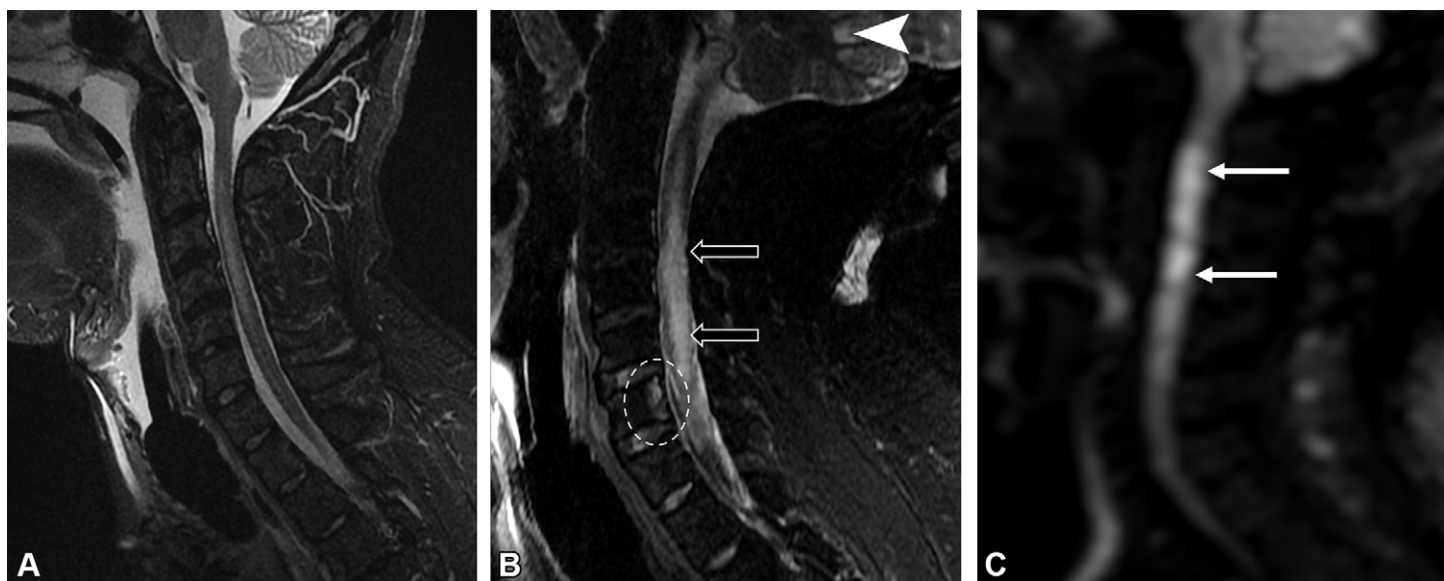


**Figure 2.** ASA infarct in a young adult with acute onset of neck pain and rapid progression to quadriplegia in less than 24 hours. **(A)** Initial sagittal T2-weighted MR image obtained 1 day after symptom onset shows long-segment hyperintense signal without cord expansion. **(B, C)** Subsequent repeat sagittal fat-saturated T2-weighted MR image **(B)** 5 days after symptom onset shows development of a vertebral body infarct (dashed oval in **B**) and increased cord edema (arrows in **B**), as well as restriction (arrows in **C**) on the sagittal diffusion-weighted image **(C)**. The patient also has small ischemic embolic infarcts in the cerebellum (arrowhead in **B**).

arteries (especially in patients with atherosclerosis). Caution should be used when designating a spinal DSA as “complete” and “negative.” Complete spinal DSA requires high technical demands and a methodical approach that often includes vertebral-level labeling, rulers, and angiographic visualization of nonselective injections (22).

### Spinal Cord Infarcts

Spinal cord infarcts have been previously reported to represent 6% of acute myelopathies, but more recent studies show spontaneous spinal cord infarcts are often misdiagnosed and likely represent 14%–16% of all patients referred for evaluation of acute transverse myelitis (5,6,23). While radiologists confidently identify classic imaging features of intracranial ischemic infarcts (think middle cerebral artery infarcts), diagnosing spinal cord infarcts proves more difficult. Drawing parallels to brain infarcts may help with regard to considering onset, symptom peak, causes, and imaging.

Acuity is paramount to accurately diagnosing spinal cord pathologic conditions (5). Noncompressive intrinsic abnormal spinal cord signal intensity can be divided into acute or nonacute pathologic findings (3,24). Acute can further be divided into hyperacute (<24 hours) or acute (1–21 days) based on when symptoms progress to their peak. The abrupt onset of symptoms and hyperacute course of cord infarcts can help differentiate spinal cord infarcts from other causes of acute intrinsic abnormal T2 spinal cord signal intensity, which include demyelinating, inflammatory, infectious, and idiopathic causes (5,24). Symptoms from spinal cord infarcts rapidly progress after onset and usually peak around 12 hours (25,26). Besides symptoms related to the specific spinal cord tract involvement, patients with cord infarcts often also have acute onset severe back pain (96%). Some infarcts can be seen with provocative maneuver such as lift-

ing a heavy object or Valsalva (25). Accurately identifying spinal cord infarcts can halt workup of other causes, spur workup for embolic disease or vasculopathy, and initiate treatment with lumbar drainage and blood pressure augmentation (although evidence is lacking for treatment effect). Correct diagnosis can also help to avoid treatments such as plasma exchange and intravenous immunoglobulin, which are harmful due to reduced cord perfusion and prothrombotic effects (25).

Causes of spinal cord infarcts include standard emboli, atherosclerosis, vasculopathies, and hypercoagulable states, as well as aortic pathologic conditions or procedures and fibrocartilaginous (disk) emboli (27). MRI features of acute and subacute infarcts overlap with features of other intrinsic spinal cord pathologic conditions. Thus, understanding acuity, symptoms, and onset are critical to distinguishing infarcts. Imaging features of spinal cord infarcts depend on location and acuity. The three most specific imaging signs of spinal cord infarcts are intramedullary diffusion restriction, vertebral body infarct (Fig 2), and concurrent vascular occlusion (25).

If imaged in the hyperacute or early acute phase, MRI findings can be normal or there may be only diffusion-weighted and subtle thin H-shaped T2 abnormalities involving the gray matter, distinguishing infarct from other pathologic conditions (7,24). Short-interval repeat imaging is warranted in suspected cases with unremarkable initial MRI examinations and can be performed beginning 2–3 days after symptom onset (25). In the acute and early subacute phase, infarcts should restrict and have MRI-evident cytotoxic edema. Thrombosed arteries and hemorrhagic transformation can have magnetic susceptibility (Fig 3). Subacute infarcts may enhance as there is break down in the blood-brain barrier, mimicking other pathologic conditions. Most infarcts are long-segment infarcts (three or more vertebral bodies).

**Figure 3.** Subacute ASA infarct from hypercoagulable state in a young adult with antiphospholipid syndrome. The patient went to bed asymptomatic and woke up paralyzed. Ten days after symptom onset following transfer from an outside hospital, the patient underwent repeat MRI. MR images show a focus of magnetic susceptibility from a clot in the ASA on the axial gradient-recalled echo image (arrowhead in **A**), enhancement of the now subacute infarct especially in the gray matter (arrow in **B**) on the axial postcontrast T1-weighted image, and intense diffusion restriction on the sagittal diffusion-weighted image (\* in **C**).

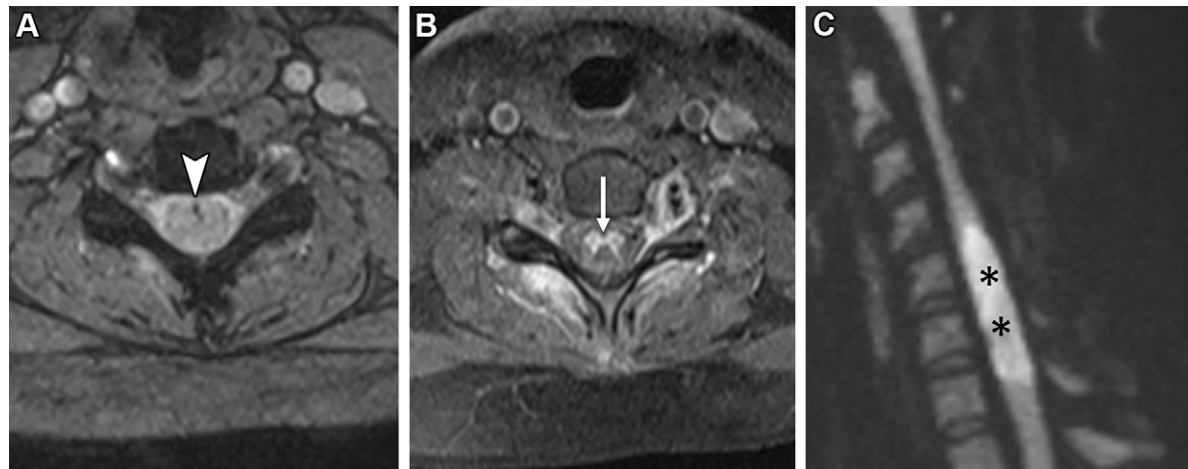
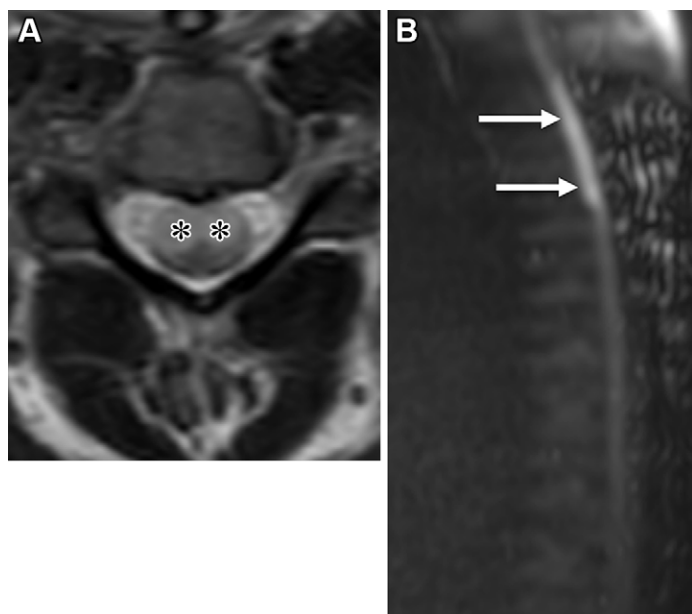


**Figure 4.** ASA infarct in a young adult with acute onset of neck pain after doing a pull-up, with rapid progression to paraplegia. **(A)** Axial T2-weighted MR image shows cytotoxic edema in the ASA territory that involves the anterior two-thirds of the spinal cord with a rounded owl's eyes appearance (\*). **(B)** Sagittal diffusion-weighted MR image shows a long segment of diffusion restriction (arrows).



Spinal cord infarcts can be territorial, watershed, or small vessel infarcts, but patterns can be difficult to appreciate due to the small size of the spinal cord. ASA infarcts involve the anterior two-thirds of the cord, with motor deficits and swollen bilateral anterior hemicords that have a characteristic “owl’s eyes” appearance (Fig 4). Collateral flow is more robust around the cord posteriorly, making the ASA territory more susceptible to ischemia (26). PSA infarcts involve the dorsal columns and lead to loss of proprioception and vibra-

tion below the level of the insult. PSA infarcts can be unilateral (Fig 5) or bilateral and have an imaging appearance that can mimic that of other causes of acute intrinsic abnormal T2 signal intensity. Differentiating factors can be an abrupt onset, infarct risk factors, and vertebral body infarcts. Vertebral body infarcts are very specific for spinal cord infarcts but are not always present. They develop days after symptom onset, are due to occlusion of the posterior vertebral body arterial branch, and result in T2-weighted imaging hyperintensity, potentially with diffusion restriction and/or enhancement (27).

## Vascular Anomalies

### Malformations versus Tumors

The ISSVA classification system, introduced by Mulliken and Glowacki in 1982 and most recently revised in May 2018, divides the umbrella term *vascular anomalies* into vascular malformations and vascular tumors in internationally consistent nomenclature (8,28). Vascular malformations are nonneoplastic structural anomalies, while vascular tumors are neoplastic proliferations of vascular endothelial cells (Table 2) (8,28,29). Malformations can occur as isolated lesions, in association with complex syndromes (29), or can be unclassified. This section focuses on three of the ISSVA simple vascular malformations: arteriovenous fistulas (AVFs), arteriovenous malformations (AVMs), and venous malformations.

### Shunting Spinal Vascular Malformations

Spinal vascular malformations can be shunting or nonshunting malformations. The two broad categories of simple shunting spinal malformations included in the ISSVA classification system are AVMs and AVFs. Shunting spinal vascular malformations are defined by their locations (intradural, dural, or epidural) and the presence of a nidus (AVM) or absence of a nidus (AVF). While knowledge of classification systems

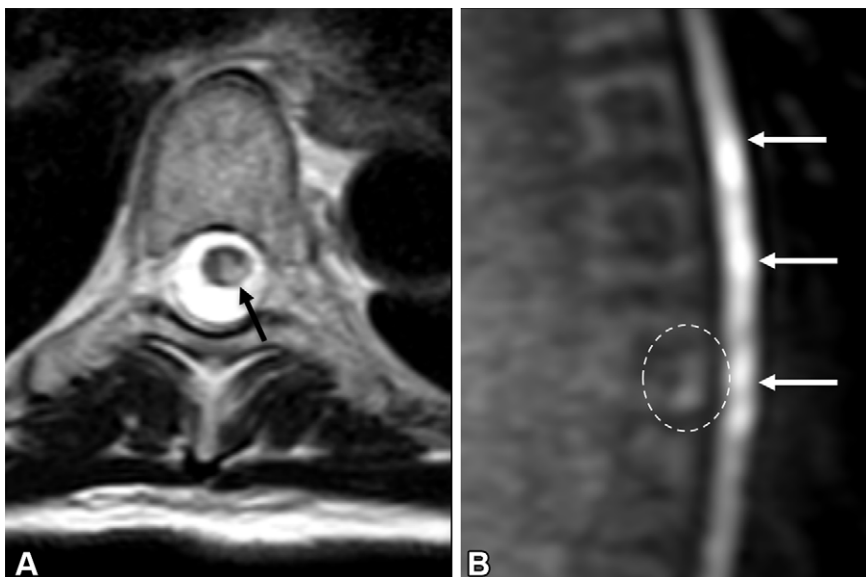


**Figure 5.** PSA infarct in an older adult with abrupt onset of pain, ataxia, and sensory disturbance. **(A)** Axial T2-weighted MR image obtained 6 days after symptom onset shows a wedge-shaped region of cytotoxic edema in the left PSA territory (arrow) that is hyperintense. **(B)** Sagittal diffusion-weighted MR image obtained 6 days after symptom onset shows that this region had a long segment of diffusion restriction (arrows). The patient also had a vertebral body infarct that was bright on the diffusion-weighted image (dashed oval in **B**) and at short inversion time inversion-recovery imaging (not shown), which developed between initial MRI (not shown) and subsequent MRI (shown here).

**Table 2: ISSVA Vascular Anomalies**

Vascular malformations

Simple:

CM

LM

VM (many VMs were previously referred to as hemangiomas; CCM is a subtype of VM)

AVM

AVF

Combined:

CM + VM

LM + VM

CM + LM + VM

CM + AVM + VM

CM + LM + AVM + VM

Of major named vessels: *channel type* or *truncal* vascular malformations

Associated with other anomalies: Klippel-Trenaunay syndrome; Sturge-Weber syndrome; CLOVES; and more

Vascular tumors

Benign: hemangiomas (including infantile and congenital)

Locally aggressive or borderline: most hemangioendotheliomas, Kaposi sarcoma

Malignant: angiosarcoma, epithelioid hemangioendothelioma

Note—AVF = arteriovenous fistula, AVM = AV malformation,

CCM = cerebral cavernous malformation, CLOVES = congenital truncal lipomatous overgrowth, vascular malformations,

epidermal nevi, scoliosis, CM = capillary malformation, LM =

lymphatic malformation, VM = venous malformation.

graphic morphology, location, and complexity (30). The most widely adopted classification scheme, based on that by DiChiuro et al (31) with subsequent additions by Heros et al (32) and most recently Takai et al (30), distinguishes between five types of shunting lesions: type I, dural AVF; type II, glomus AVM; type III, juvenile AVM; type IV, perimedullary AVF; and type V, epidural AVF. Yet each shunting lesion, distinguished based on location (dural, intradural, or epidural) of the pathologic connection and presence of a nidus (AVM when nidus is present), should be considered separate diseases with distinctive pathophysiology, symptoms, treatment, and prognosis and are discussed in the following sections as such (Table 3).

**Arteriovenous Fistulas.**—Spinal dural AVF, also known as intradural dorsal AVF, is a fistulous connection with no nidus between a radicular artery and radicular vein located at the dura, within the nerve root dural sleeve at an intervertebral foramen. It is the most common type (up to 70%) of spinal vascular shunt, most often located at the thoracolumbar junction. Characteristic progressive myelopathic symptoms (Foix-Alajouanine syndrome) in older adults and imaging findings are secondary to spinal cord venous congestion, as arterialized blood refluxes into the perimedullary and longitudinal cord veins and the radiculomedullary venous system gradually fails. MRI findings reveal serpiginous perimedullary flow voids typically dorsal to the cord, corresponding to enlarged congested spinal cord veins (Fig 6). Cord edema typically begins caudally near the conus, unrelated in location to the inciting fistula. Enhancement may also be present, which can confuse radiologists and contribute to a delay in diagnosis. In patients with missed or delayed spinal dural AVF diagnoses, around 80% have enhancement, 96% have intramedullary edema, and 96% have a prominent intradural vessel (4). The fistulous connection and early filling radicular vein can be localized at first-pass MRA or TR-MRA. Treatment is aimed at disconnecting the fistulous site, either surgically or endovascularly.

Pial AVF, also known as perimedullary or intradural ventral AVF, is a fistulous connection with no nidus between

for AVMs and AVFs is beneficial, the most important thing for diagnostic radiologists to do is raise suspicion of shunting malformations, provide detailed descriptions of imaging findings, and recommend appropriate next steps.

**Most Common Classifications.**—Multiple schemes have been proposed to classify spinal vascular shunts based on angio-

**Table 3: Shunting Spinal Vascular Malformations**

Parameter	Location of Pathologic Connection			
	Intradural	Dural	Epidural	Extraspinal or Metameric
No nidus (AVF)	Pial AVF	Dural AVF	Epidural AVF	...
With nidus (AVM)	Intramedullary AVM	...	...	Metameric AVM

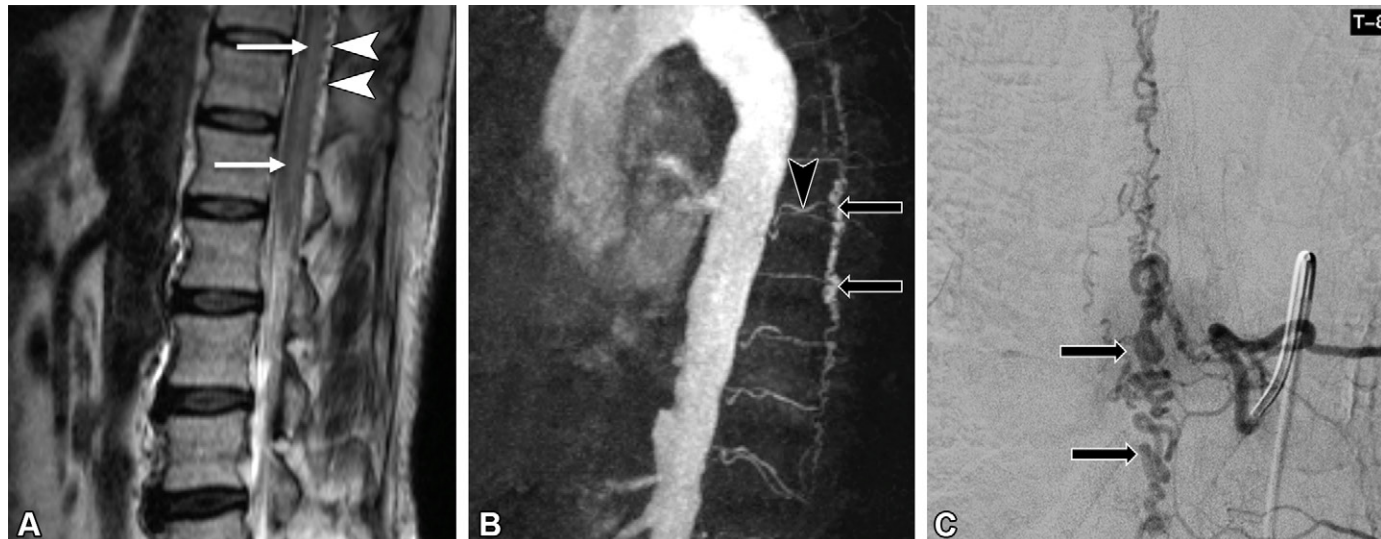


**Figure 6.** Dural AVF in an older man with slowly progressing subacute lower extremity weakness. **(A)** Sagittal T2-weighted image centered at the thoracolumbar junction shows edema in the lower thoracic spinal cord and conus medullaris (arrows) and multiple tiny but pathologically enlarged dorsal T2-hypointense flow voids (arrowheads). **(B)** TR-MRA three-dimensional reformation in the lateral view shows the enlarged intradural veins (arrows) and raises suspicion for a T8-level feeding segmental artery (arrowhead in **B**). **(C)** DSA image shows that the left T8 was the first selected segmental artery and confirms the shunt and early filling of dilated intradural veins (arrows).

spinal cord arteries (ASA and/or PSA) and veins located on the pial (spinal cord) surface (Fig 7), ranging in size and complexity from single artery-to-vein connection to multiple arterial feeders. Prevalence is estimated to be 8%–19% of spinal vascular malformations, with complex fistulas more likely associated with genetic syndromes including Parkes Weber syndrome, capillary malformation–arteriovenous malformation (CM-AVM) syndrome, and hereditary hemorrhagic telangiectasia (33). Most patients are symptomatic, and approximately two-thirds of which present with spinal venous congestion akin to dural AVF. However, the higher flow, particularly in more complex lesions, predisposes to spinal hemorrhage in one-third of symptomatic patients. T2-weighted imaging reveals prominent perimedullary flow voids, more commonly along the ventral cord, with variable findings of cord edema and enhancement.

Epidural AVF, also known as extradural fistula, is a high-flow fistulous connection with no nidus between the epidural arterial arcade and epidural venous plexus, typically a dilated epidural venous pouch (Fig 8) without a nidus. Patients may be asymptomatic if the shunted flow is adequately routed via the extensive anastomosis to the paraspinal venous system. They will become symptomatic from cord compression secondary to an engorged epidural venous plexus (Fig 9) or when extraspinal venous outflow is insufficient or is occluded, re-

sulting in reflux into the cord veins with cord venous congestion. T2-weighted imaging findings often demonstrate the dilated epidural venous pouch, most often located in the ventral epidural space, small adjacent flow voids, and findings of cord venous congestion, if present. The adjacent flow voids can raise suspicion of vascular malformation and differentiate epidural AVF from meningioma or nerve sheath tumors. Endovascular treatment is generally safer and more feasible than surgical obliteration.

**Arteriovenous Malformations.**—Intramedullary AVM, also known as glomus or intradural AVM, is a pathologic shunt between spinal cord arteries (typically ASA) and spinal cord veins with an intervening intramedullary or pial-based nidus (Fig 10). Like pial AVFs, intramedullary AVMs have associations with specific genetic disorders. Intramedullary AVMs are high-flow lesions with a propensity for hemorrhage. Less commonly, spontaneous venous thrombosis can cause acute deterioration, and reflux of arterialized blood to the longitudinal cord veins can cause venous congestion. Arterialized dilated venous outflow appear as prominent intramedullary, perimedullary, or epidural flow voids at MRI with early filling at MRA. The nidus is usually eccentric within or partially within the spinal cord, with surrounding intramedullary T2-hyperintense gliosis, edema, or ischemia. Nidal aneurysms are frequently observed,

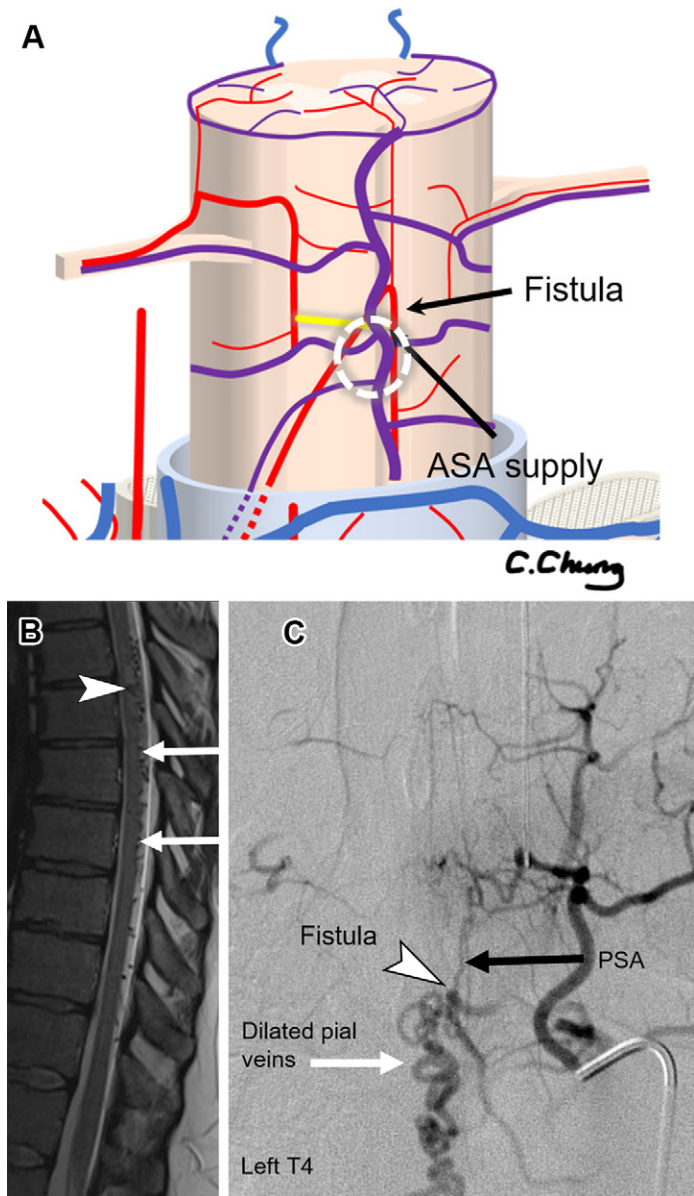


**Figure 7.** Pial AVF. **(A)** Diagram shows a fistulous connection along the pial surface between the ASA and pial vein (dashed oval). **(B)** Sagittal T2-weighted MR image of the thoracic spine in a young adult with a dorsal pial AVF shows multiple extramedullary intradural flow voids from tortuous dilated veins (arrows) due to arteriovenous shunting and focal void projecting into the spinal cord (arrowhead) with surrounding edema, localizing the AVF to the dorsal high thoracic spinal cord. **(C)** DSA image of the selected left T4 injection shows the fistula (arrowhead) from the PSA (black arrow).

with rupture causing intramedullary and/or subarachnoid hemorrhage with associated mass effect.

Metameric AVMs (also called juvenile AVM, intradural-extradural AVM, or Cobb syndrome) are diffuse highly vascular AVMs with an intramedullary nidus also involving extraspinal structures (bony spine, paraspinal soft tissues, and skin from the same metameric level). Patients may be asymptomatic or can present with acute hemorrhage or progressive neurologic deficit. Imaging demonstrates flow voids in the intradural space, paraspinal tissues, and extraspinal tissues with mass effect on the cord (Fig 11). Extensive soft-tissue involve-

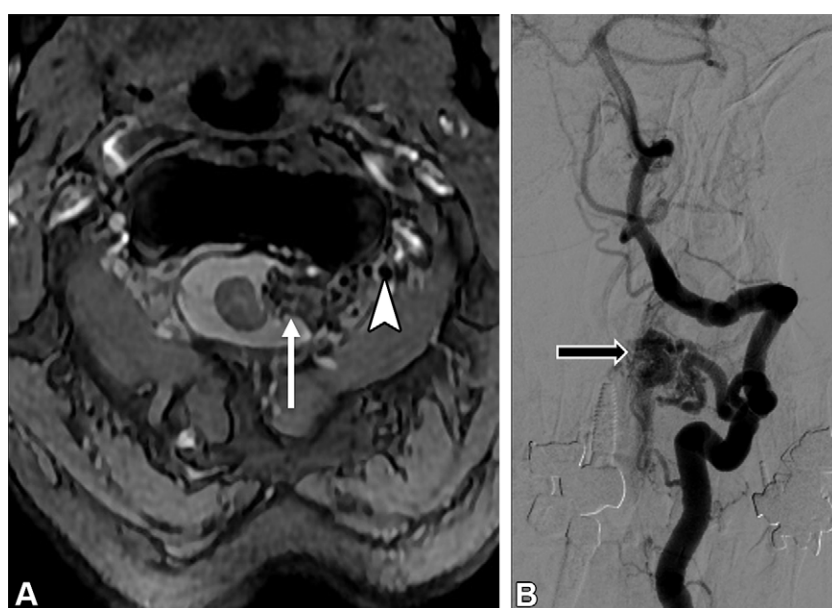
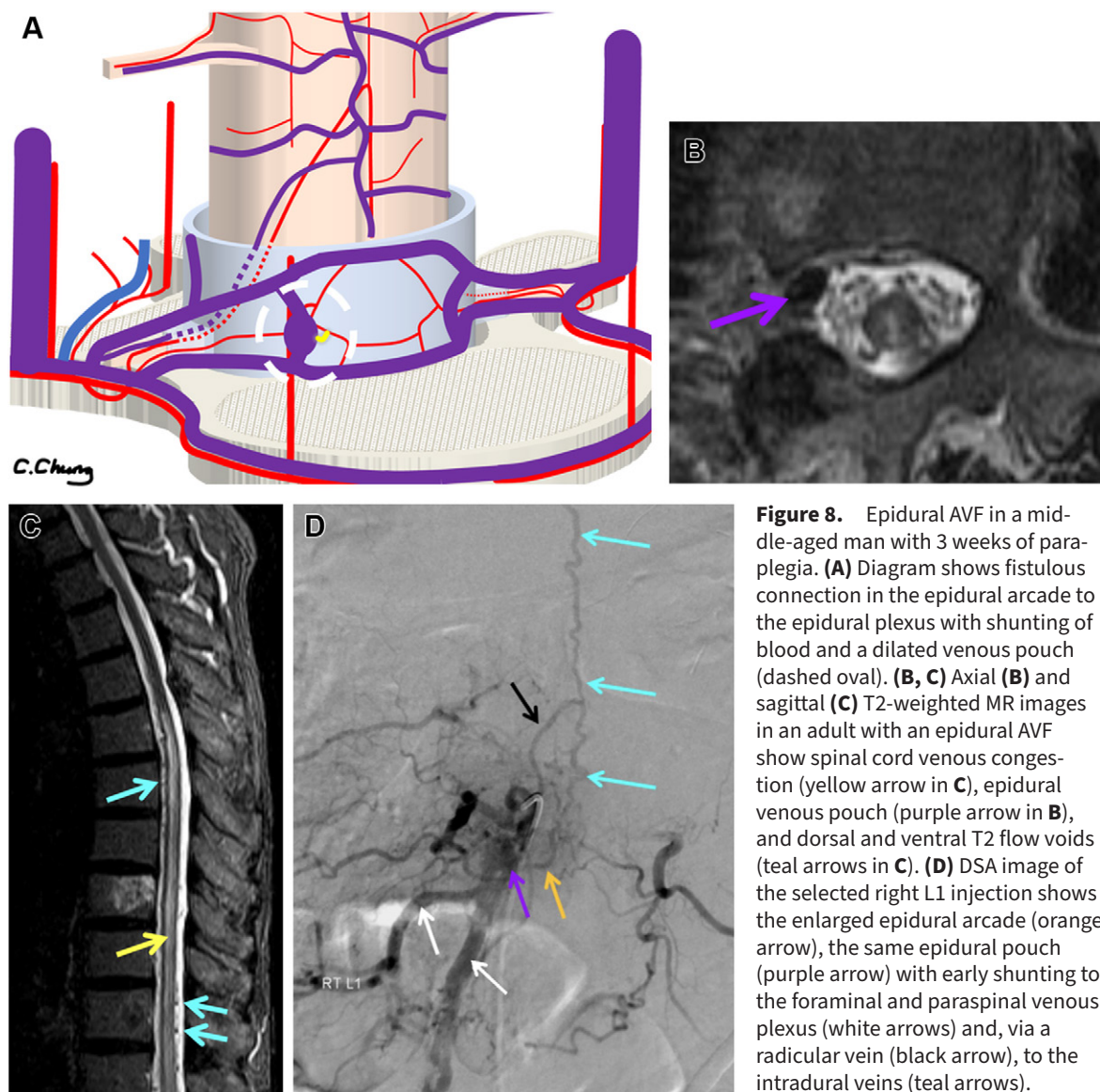
ment may resemble a mass lesion at MRI. Multidisciplinary management with staged, possibly palliative, treatment is generally undertaken, as complete resection is difficult with much risk of neurologic deficit.

### Nonshunting Spinal Vascular Malformations

Venous malformations are the most common type of slow-flow nonshunting simple vascular malformations. They are known by many names. Pathologic conditions termed *cavernous malformation*, *cavernoma*, *cavernous hemangioma*, *epidural hemangioma*, and *intraosseous hemangioma* are all actually slow-flow venous malformations. Adoption of this terminology has been inconsistent. Many radiologists and clinicians continue to refer to older terms and are often confused by newer terms. For this reason, some recommend dictating the new nomenclature first followed by previous nomenclature in parentheses, for example, “venous malformation (previously known as hemangioma)” (34,35). Since cerebral cavernous malformation is a type of simple venous malformation per ISSVA classifications (8), the term *spinal cord cavernous malformation* (SCCM) will be used in this article when referring to spinal location of that particular entity.

SCCMs account for 5%–12% of all spinal vascular lesions. They are characterized by a compact focus with abnormal dilated vascular spaces (nonneoplastic endothelial-lined caverns) that have no intervening neural tissues (36). An SCCM may become clinically apparent with acute onset of neurologic deficit following an acute intramedullary hemorrhage with mass effect. Repetitive intralesional microhemorrhages can lead to lesion enlargement and characteristic hemosiderin deposition in and around the lesion. Imaging features of SCCMs are like those found in the brain. At MRI, they show central heterogeneous T1- and T2-weighted hyperintensity with a peripheral hypointense halo due to hemosiderin deposition resulting in a “chocolate-covered popcorn” appearance at T2-weighted imaging (Fig 12) and gradient-recalled echo and susceptibility-weighted imaging. SCCMs have variable enhancement and are not evident at DSA. Occasionally, they are intimately associated with a developmental venous anomaly.

They can be a single sporadic lesion or multiple familial lesions (cerebral cavernous malformation gene locus) (8). Although once thought of as a developmental disorder, the de novo appearance of cavernous malformations has been firmly established, most notably after radiation therapy (37). Radiation-induced cavernous malformations can be within the spinal cord or along the cauda equina nerve roots where they mimic leptomeningeal disease (Fig 13) (38,39). Negative cerebrospinal fluid studies, stability over time, thick radiation scars, and lack of central nervous system findings outside of the radiation field can differentiate small cauda equina malformations from leptomeningeal disease (40). Treatment options include surgery and radiation for intracranial lesions, but the treatment chosen depends on multiple factors such as clinical manifestation, location, and number of hemorrhagic events. However, for SCCMs, some authors favor microsurgery with intraoperative neurophysiologic monitoring over other conservative treatments (41).



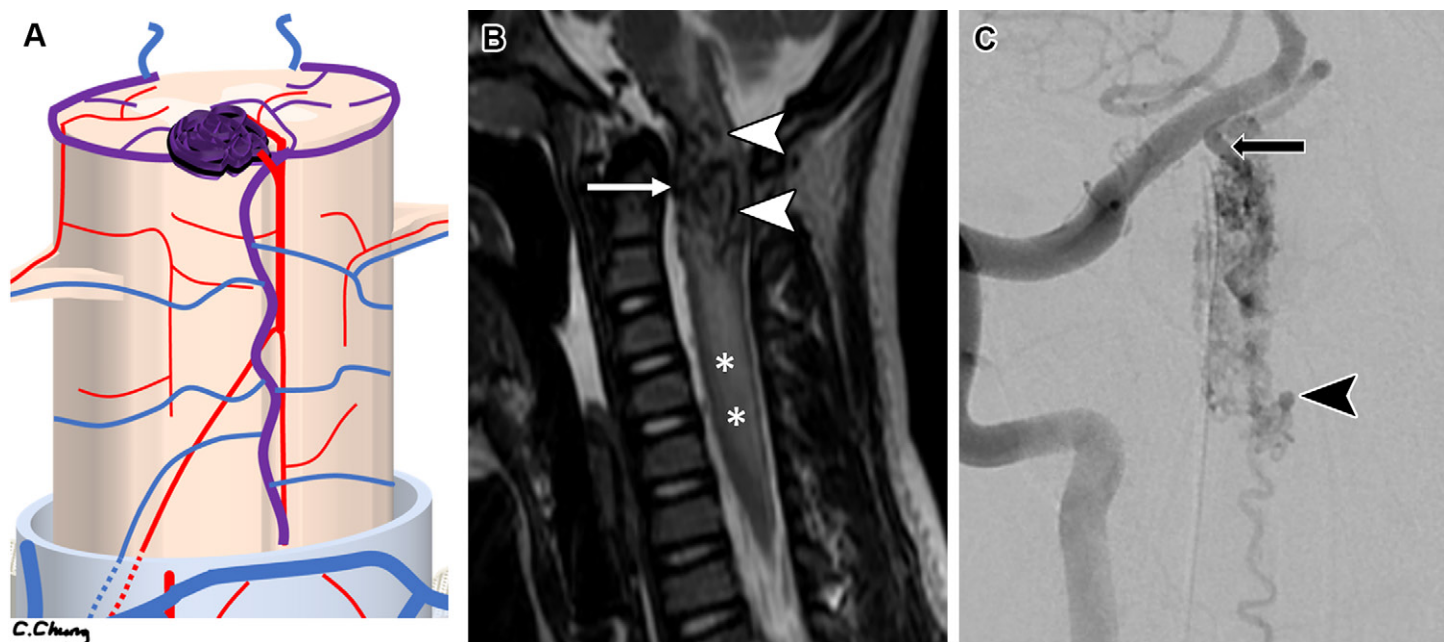


**Figure 10.** Intramedullary glomus AVM. **(A)** Diagram shows the intramedullary vascular nidus near the surface of the spinal cord, supplied by the ASA, and shunting blood (purple) that drains to the enlarged anterior spinal vein. **(B)** Sagittal T2-weighted MR image of the cervical spinal cord in a child who presented with acute onset of weakness due to AVM rupture and hematomyelia shows a tangle of vessels within the spinal cord with hypointense flow voids (arrowheads), suspected ventral feeding and draining vessels (arrow), and surrounding edema (\*). **(C)** DSA image with injection of the right vertebral artery shows the AVM nidus supplied by an enlarged ASA (arrow) and associated intranidal aneurysm (arrowhead).

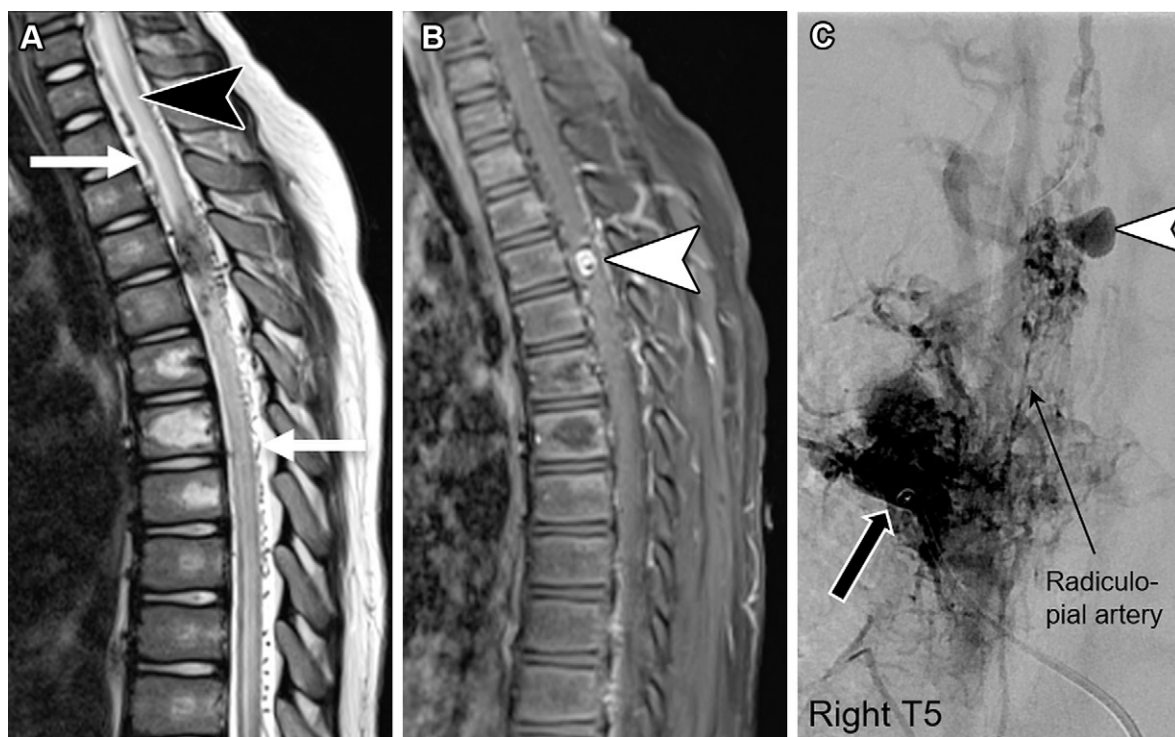


**Figure 11.** Metameric (juvenile) AVM. **(A, B)** Sagittal T2-weighted **(A)** and postcontrast T1-weighted **(B)** MR images in a child show an intramedullary component to the AVM with an intranidal aneurysm (arrowhead in **B**), surrounding edema (arrowhead in **A**), and T2 hypointense flow voids (arrows in **A**). **(C)** DSA image with a selected right T5 injection shows the extensive extraspinal component (thick black arrow) as well as the intramedullary nidus with intranidal aneurysm (arrowhead).

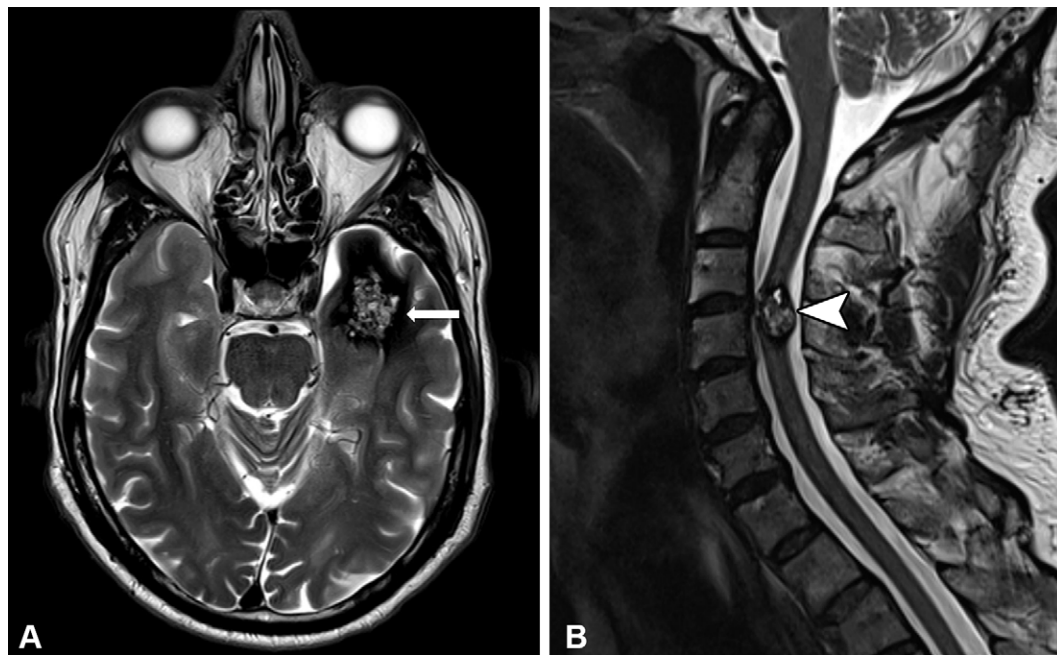


**Figure 12.** Patient with both cerebral and spinal cord cavernous malformations. **(A)** Axial T2-weighted MR image of the brain shows an intra-axial heterogeneous left anterior temporal lobe lesion with small central hyperintense foci and a peripheral hypointense halo of hemosiderin (arrow), with the typical appearance of chocolate-covered popcorn. **(B)** Sagittal T2-weighted MR image of the cervical spine in the same patient also shows an intramedullary lesion with the same imaging characteristics (arrowhead).



**Figure 13.** Radiation-induced cavernous malformations in a patient with radiculopathy and a history of remote prior radiation therapy for testicular cancer. Sagittal postcontrast T1-weighted MR image of the lumbar spine shows multiple small enhancing nodular lesions along the cauda equina (arrows) with associated faint diffuse cauda equina enhancement and very thick clinically and imaging-evident burn (\*).

## Other Lesions

**Spinal Aneurysms.**—While aneurysms involving spinal cord arteries are generally seen in the setting of spinal AVMs or fistulas, approximately half exist as an isolated finding (42), typically a fusiform aneurysm of the ascending intradural portion of a radiculopial or radiculomedullary artery at the thoracic or cervical levels. A ruptured spinal artery aneurysm

causes sudden onset back pain and myelopathic symptoms due to cord compression. Spinal artery aneurysms represent a rare but underrecognized cause of cryptogenic spinal intradural or subarachnoid hemorrhage. Blood products are characteristically centered lateral to the cord in the earlier stages (Fig 14), although they can extend to the skull base and infrequently the spinal subdural space. Rarely, thrombosis and distal emboli from an unruptured aneurysm result in cord infarct, particularly if it involves the artery of Adamkiewicz (43). DSA is the reference standard for diagnosis, although post-contrast noninvasive imaging may help reveal an enhancing aneurysm. Natural history is generally favorable with spontaneous aneurysm thrombosis and low rebleeding risk, although early fatal rebleeding has been reported (44). When technically feasible, surgical or endovascular treatment is generally safe and effective.

**Cerebrospinal Fluid Venous Fistula.**—Cerebrospinal fluid venous fistula (CVF) is an abnormal connection between the spinal subarachnoid space and an adjacent paraspinal vein that allows shunting of cerebrospinal fluid and results in spontaneous intracranial hypotension. MRI brain findings indicating spontaneous intracranial hypotension include dural enhancement, venous distention, enlarged pituitary, brainstem sagging, and subdural fluid collections (Fig 15). At least one MRI sign of spontaneous intracranial hypotension was present in up to 91% of cases (45,46). CVF is a relatively recently recognized cause of spontaneous intracranial hypotension, first described in 2014. It should be considered when there is no evidence of extradural fluid (cerebrospinal fluid) on MR or CT myelograms. CVFs are often anatomically associated with a diverticulum of a nerve root sleeve, with the fistulous connection commonly originating from the diverticulum itself (up to 82%) (47). Arachnoid granulations are responsible for cerebrospinal fluid absorption and have been found to have an increased presence along spinal nerve roots, particularly in the mid and

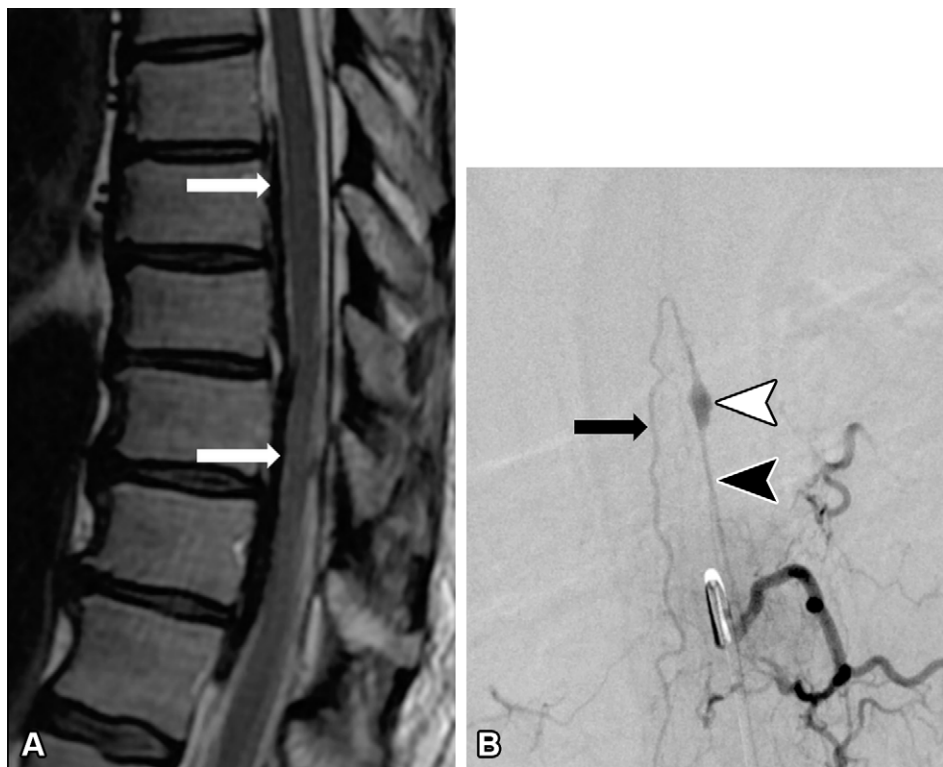


**Figure 14.** Recently ruptured spinal artery aneurysm in an adult who presented with acute back pain. **(A)** Sagittal T2-weighted MR image shows acute subarachnoid hemorrhage (arrows) with sentinel clot in the ventral spinal canal. **(B)** Subsequent DSA injection image of the left T12 segmental artery shows the aneurysm (white arrowhead) of the artery of Adamkiewicz (black arrowhead) supplying the ASA (arrow). The fusiform appearance and the location suggest a dissecting aneurysm.

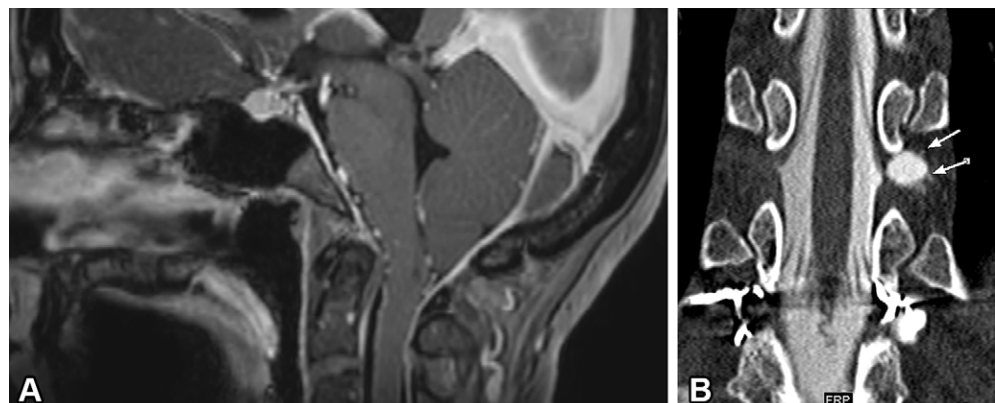


**Figure 15.** CVF in a patient presenting with spontaneous intracranial hypotension. **(A)** Sagittal postcontrast T1-weighted MR image of the brain shows findings of intracranial hypotension, which include sagging of the brain, pachymeningeal enhancement, distention of venous sinuses, and an enlarged pituitary gland. **(B)** Coronal CT myelogram of the lower thoracic spine shows a nerve root diverticulum with curvilinear paraspinal contrast media within a vein, indicating a CVF (arrows). This patient had previous CVFs and embolizations at the level below.

lower thoracic spine. It has been hypothesized that a rupture of a granulation may be the inciting event for a CVF (46).

CT myelography is the initial invasive investigation of choice in patients suspected of having a CVF. The most specific sign of a CVF is the opacification of epidural or paravertebral veins at CT myelography (Fig 15). Identification of renal excretion of contrast media is a secondary sign of venous shunting. Specialized techniques such as decubitus CT myelography and decubitus digital subtraction myelography improve the accuracy of diagnosing CVFs in patients with spontaneous intracranial hypotension with negative conventional CT myelography (46,48). CVF can be treated surgically or with endovascular venous embolization.

## Tumors

### Vascular Tumors

Per ISSVA classification, vascular tumors are characterized by neoplastic endothelial proliferation and can be benign, locally aggressive, or malignant (Table 2) (8). True hemangiomas are benign neoplastic vascular tumors. They can be infantile or congenital and are cutaneous lesions with distinct growth and regression patterns. Infantile hemangiomas are histologically positive for glucose transporter 1 (GLUT-1) (8). Hemangiomas avidly enhance and are hyperintense at T2-weighted imaging but are slightly less hyperintense at T2-weighted imaging than venous malformations (49). Hemangiomas should

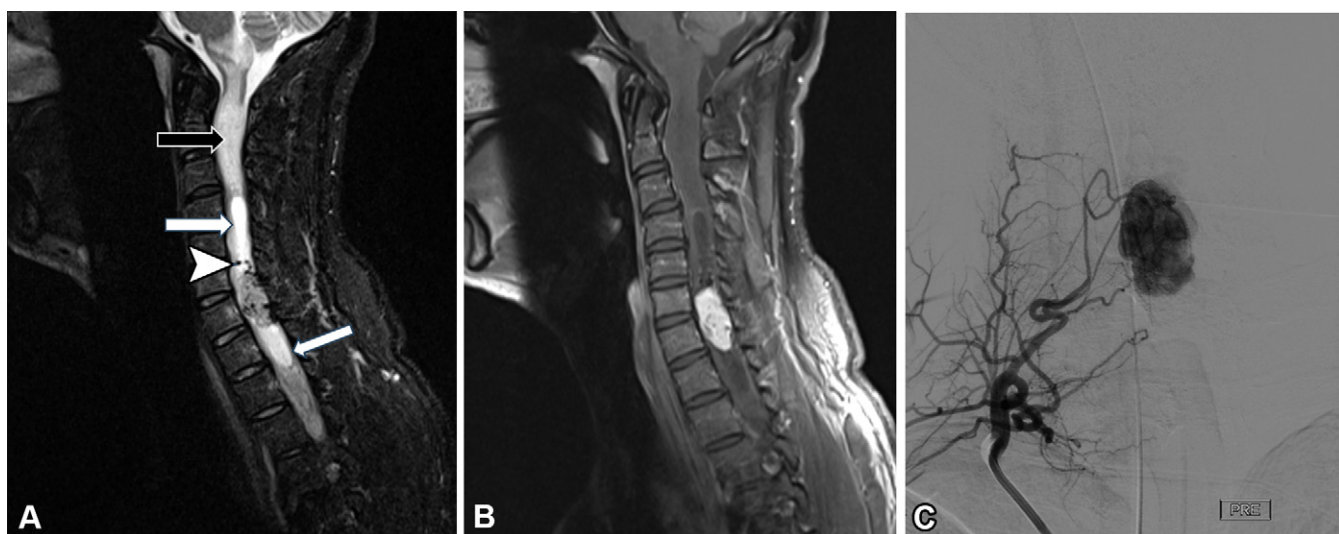


**Figure 16.** Spinal hemangioblastoma in a patient with an intramedullary mass in the mid cervical spine. **(A)** Sagittal T2-weighted MR image shows that the intramedullary mass has cysts extending cephalic and caudal to the lesion (white arrows), multiple adjacent flow voids (arrowhead), and surrounding spinal cord edema (black arrow). **(B)** Sagittal postcontrast T1-weighted MR image shows the lesion with intense homogeneous rounded masslike enhancement that is much smaller than the extent of surrounding edema. **(C)** DSA injection image of the thyrocervical trunk shows the high vascularity of this mass before preoperative embolization.

be lobular and well circumscribed. These may involve the soft tissues near the spine. Locally aggressive, borderline malignant, or malignant vascular tumors have a higher propensity to involve deeper tissues in and around the spinal canal. Irregular margins and atypical signal intensity expand the differential diagnosis. A biopsy can be warranted whenever other aggressive or malignant lesions such as rhabdomyosarcoma, angiosarcoma, or kaposiform hemangioendothelioma are suspected (50).

### Hypervascular Masses

While not true vascular tumors, some neoplastic masses in and around the spinal cord can be hypervascular and have associated shunting. These include but are not limited to hemangioblastoma, solitary fibrous tumors, paragangliomas, and metastases. Treatment depends on multiple factors, including neurologic, oncologic, mechanical, and systemic considerations (NOMS) and spine instability neoplastic score (SINS) for vertebral metastases (51). For hypervascular masses, DSA embolization can be therapeutic or performed preoperatively to reduce blood loss. TR-MRA aids in distinguishing hypervascular from nonhypervascular spinal lesions, decreasing futile DSA examinations (52).

Hemangioblastomas are hypervascular World Health Organization grade 1 non-neuroepithelial mesenchymal tumors (1). They can be associated with Von Hippel-Lindau disease (20%) or can occur sporadically (80%) (53) and typically manifest in young adults. More than 50% are at or near the pial surface (54). They demonstrate intense homogeneous enhancement due to the tumor's high vascularity and are frequently accompanied by a surrounding cyst or syrinx that is much larger than the enhancing lesion (Fig 16). The presence of flow voids at T2-weighted imaging surrounding the lesion can aid in diagnosis. Cord edema can be from arteriovenous shunting, venous congestion, and/or tumor inflammatory

factors. Manifestation varies and can include cystic or syrinx-related signs, diffuse spinal cord enlargement, exophytic growth, or even extramedullary symptoms (55). Preoperative embolization is often beneficial.

Solitary fibrous tumors (some of which were previously known as hemangiopericytomas) are rare, comprising less than 1% of all central nervous system tumors. They are found more commonly in the brain than in the spinal canal, where the dorsal cervical region is the most common site (56). They are considered grade II or III (anaplastic) based on the mitotic index (57). Lesions are typically intradural extramedullary, but intramedullary, extradural, and multicompartimental involvement can occur. Additionally, there can be substantial extension outside the spinal canal, sometimes with bony remodeling. At MRI, solitary fibrous tumors are isointense or bright at T2-weighted imaging and are generally enhancing, although to varying degrees. Hypervascularity, sometimes with substantial angiographic shunting (Fig 17), can create a salt-and-pepper appearance at MRI similar to that of paragangliomas and have associated enlarged adjacent flow voids. Surgical resection is the mainstay of treatment with adjuvant radiation therapy often suggested for higher grade or recurrent lesions (56,58).

Lastly, metastases are more commonly seen hypervascular spinal tumors. Intramedullary metastases are less common than osseous metastases and can have tumoral enhancement and marked surrounding vasogenic edema, just like those in the brain. Characteristic rim and flame signs are described specific features of spinal cord metastases (Fig 18) (59). Extradural hypervascular spinal metastases include renal cell carcinoma, hepatocellular carcinoma, thyroid carcinoma, and primary bone tumors such as plasmacytoma. Up to two-thirds of renal cell carcinoma metastases are hypervascular. Renal cell carcinoma spinal metastases most commonly manifest with pathologic fractures, often with cord compres-

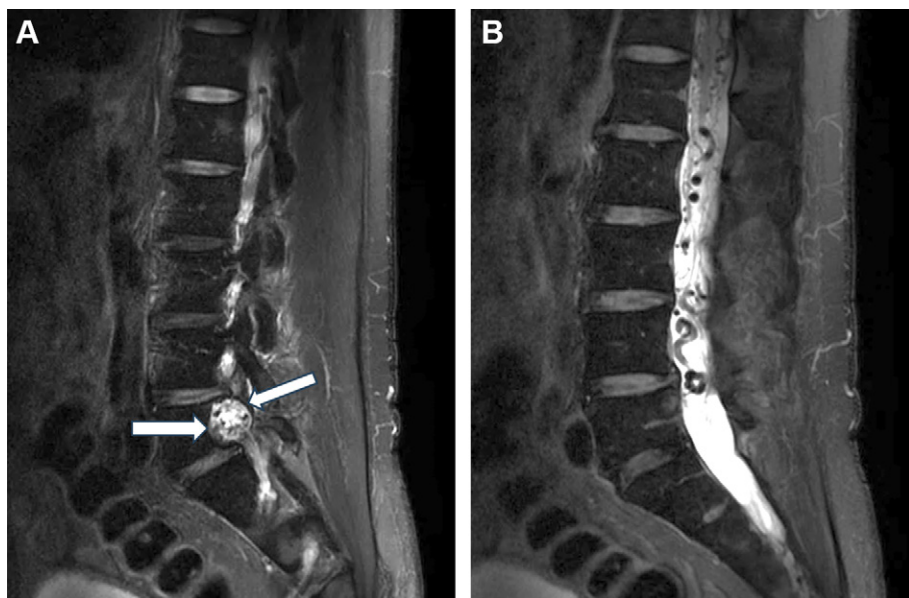


**Figure 17.** Shunting solitary fibrous tumor in an adult. **(A)** Parasagittal T2-weighted MR image of the lumbar spine shows a hemangiopericytoma (arrows) occupying the right L5 neural foramen. The lesion is hyperintense with visible low-signal-intensity flow voids and is remodeling the posterior margin of L5. **(B)** Midline sagittal MR image shows extensive enlarged perimedullary draining veins.

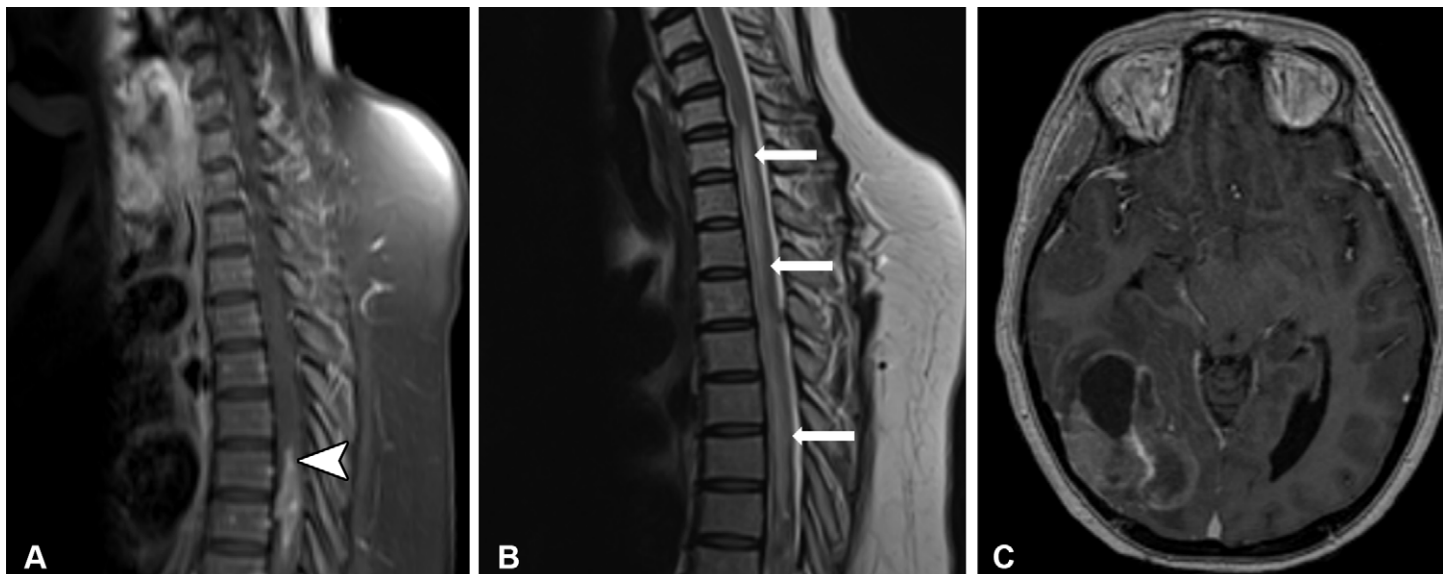


**Figure 18.** Intramedullary metastasis in an adult woman with breast cancer and intracranial metastases. **(A, B)** Sagittal postcontrast T1-weighted MR image **(A)** shows an intramedullary mass with enhancement with a rim sign of more hyperintense peripheral enhancement and a flame sign of tapered cranial (arrowhead in **A**) and caudal ends. Just like intracranial metastases, there is associated hyperintense vasogenic edema (arrows in **B**) that can extend far beyond tumor margins on the sagittal T2-weighted MR image **(B)**. **(C)** Axial T1-weighted MR image shows a large heterogeneously enhancing right temporo-occipital junction metastasis.

sion (60). Conventional MRI may help to show large T2-hyperintense flow voids associated with the vertebral lesions (Fig 19). Radiologists should include such findings in their reports to alert the surgeons, especially in patients with unknown primary tumors. Shunting metastases should be treated like AVMs as operative blood loss can be very high (up to 5 L in renal cell carcinoma metastases) and is reduced by preoperative embolization (61).

## Conclusion

Vascular pathologic conditions in and around the spinal cord have a broad range of causes that can be divided into infarcts, anomalies, and tumors. While spinal pathologic entities and imaging findings can be small, they often mirror those in the

brain. Radiologists armed with a solid foundation of knowledge, specific spine imaging protocols, and a high level of suspicion can aid in the accurate and timely diagnosis of spinal vascular pathologic conditions.

**Author affiliations.**—From the Department of Diagnostic and Interventional Imaging, Division of Neuroradiology, UTHealth Houston, 6431 Fannin St, MSB 2.130, Houston, TX (J.M.); Department of Radiology and Neurosurgery, NYU Langone Health, New York, NY (C.C., E.R., M.S.); and Department of Diagnostic and Interventional Imaging, Division of Neuroradiology (R.S., C.S., E.B., R.R., J.G.H.) and Department of Neurosurgery (P.R.C.), UTHealth Houston, Houston, Tex. Presented as an education exhibit at the 2023 RSNA Annual Meeting. Received March 8, 2024; revision requested April 9 and received April 17; accepted April 29. **Address correspondence to** J.M. (email: jennifer.l.mccarty@uth.tmc.edu).

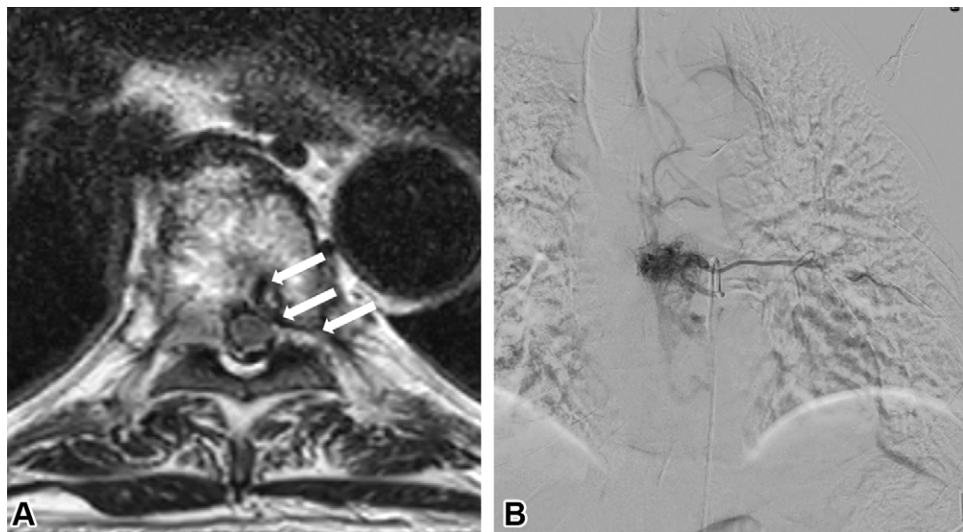


**Figure 19.** Renal cell carcinoma osseous vertebral body metastasis in an adult. **(A)** Axial T2-weighted MR image shows the hyperintense lesion in the body and right pedicle of a midthoracic vertebra. There is a large left posterior vertebral body and ventral epidural flow void (arrows) and some extension to the epidural space. **(B)** DSA image with segmental arterial injection shows a dense tumor blush and rapid filling of epidural veins. The lesion was subsequently embolized.

**Disclosures of conflicts of interest.**—The authors, editor, and reviewers have disclosed no relevant relationships.

## References

- Shih RY, Koeller KK. Intramedullary Masses of the Spinal Cord: Radiologic-Pathologic Correlation. *RadioGraphics* 2020;40(4):1125–1145.
- Eisenmenger LB, Peret A, Roberts GS, et al. Focused Abbreviated Survey MRI Protocols for Brain and Spine Imaging. *RadioGraphics* 2023;43(6):e220147.
- Lee MJ, Aronberg R, Manganaro MS, Ibrahim M, Parmar HA. Diagnostic Approach to Intrinsic Abnormality of Spinal Cord Signal Intensity. *RadioGraphics* 2019;39(6):1824–1839.
- Brinjikji W, Nasr DM, Morris JM, Rabinstein AA, Lanzino G. Clinical Outcomes of Patients with Delayed Diagnosis of Spinal Dural Arteriovenous Fistulas. *AJNR Am J Neuroradiol* 2016;37(2):380–386.
- Barrera P, Fitzgerald KC, Mealy MA, et al. Clinical biomarkers differentiate myelitis from vascular and other causes of myelopathy. *Neurology* 2018;90(1):e12–e21.
- Zalewski NL, Flanagan EP, Keegan BM. Evaluation of idiopathic transverse myelitis revealing specific myelopathy diagnoses. *Neurology* 2018;90(2):e96–e102.
- Peckham ME, Hutchins TA. Imaging of Vascular Disorders of the Spine. *Radioclim North Am* 2019;57(2):307–318.
- ISSVA classification for vascular anomalies. International Society for the Study of Vascular Anomalies. <https://www.issva.org/UserFiles/file/ISSVA-Classification-2018.pdf>. Published April 2014. Updated May 2018. Accessed July 1, 2023.
- Kona MP, Buch K, Singh J, Rohatgi S. Spinal Vascular Shunts: A Patterned Approach. *AJNR Am J Neuroradiol* 2021;42(12):2110–2118.
- Gunnal SA, Farooqui MS, Wabale RN. Study of Middle Cerebral Artery in Human Cadaveric Brain. *Ann Indian Acad Neurol* 2019;22(2):187–194.
- Rai AT, Hogg JP, Cline B, Hobbs G. Cerebrovascular geometry in the anterior circulation: an analysis of diameter, length and the vessel taper. *J Neurointerv Surg* 2013;5(4):371–375.
- Shapiro M. Spinal Arterial Anatomy. <http://neuroangio.org/spinal-vascular-anatomy/spinal-arterial-anatomy/>. Published 2024. Accessed July 1, 2023.
- Vargas MI, Gariani J, Sztajzel R, et al. Spinal cord ischemia: practical imaging tips, pearls, and pitfalls. *AJNR Am J Neuroradiol* 2015;36(5):825–830.
- Yoshioka K, Niiuma H, Ehara S, Nakajima T, Nakamura M, Kawazoe K. MR angiography and CT angiography of the artery of Adamkiewicz: state of the art. *RadioGraphics* 2006;26(Suppl 1):S63–S73.
- Yang H, Qi YY, Gong MF, et al. CT angiography of cervical anterior spinal artery and anterior radicular artery: preliminary study on technology and its clinical application. *Clin Imaging* 2015;39(1):32–36.
- Hu X, Yuan Z, Liang K, et al. Application of Spinal Subtraction and Bone Background Fusion CTA in the Accurate Diagnosis and Evaluation of Spinal Vascular Malformations. *AJNR Am J Neuroradiol* 2024;45(3):351–357.
- Shimoyama S, Nishii T, Watanabe Y, et al. Advantages of 70-kV CT Angiography for the Visualization of the Adamkiewicz Artery: Comparison with 120-kV Imaging. *AJNR Am J Neuroradiol* 2017;38(12):2399–2405.
- Almansour H, Herrmann J, Gassenmaier S, et al. Deep Learning Reconstruction for Accelerated Spine MRI: Prospective Analysis of Interchangeability. *Radioiology* 2023;306(3):e212922.
- Kannath SK, Mandapalu S, Thomas B, Enakshy Rajan J, Kesavadas C. Comparative Analysis of Volumetric High-Resolution Heavily T2-Weighted MRI and Time-Resolved Contrast-Enhanced MRA in the Evaluation of Spinal Vascular Malformations. *AJNR Am J Neuroradiol* 2019;40(9):1601–1606.
- Amarouche M, Hart JL, Siddiqui A, Hampton T, Walsh DC. Time-resolved contrast-enhanced MR angiography of spinal vascular malformations. *AJNR Am J Neuroradiol* 2015;36(2):417–422.
- Grossberg JA, Howard BM, Saindane AM. The use of contrast-enhanced, time-resolved magnetic resonance angiography in cerebrovascular pathology. *Neurosurg Focus* 2019;47(6):E3.
- Barrera P, Heck D, Greenberg B, Wolinsky JP, Pardo CA, Gailloud P. Analysis of 30 Spinal Angiograms Falsey Reported as Normal in 18 Patients with Subsequently Documented Spinal Vascular Malformations. *AJNR Am J Neuroradiol* 2017;38(9):1814–1819.
- Sandson TA, Friedman JH. Spinal cord infarction. Report of 8 cases and review of the literature. *Medicine (Baltimore)* 1989;68(5):282–292.
- Kranz PG, Amrhein TJ. Imaging Approach to Myelopathy: Acute, Subacute, and Chronic. *Radioclim North Am* 2019;57(2):257–279.
- Zalewski NL, Rabinstein AA, Krecke KN, et al. Characteristics of Spontaneous Spinal Cord Infarction and Proposed Diagnostic Criteria. *JAMA Neurol* 2019;76(1):56–63.
- Zalewski NL, Rabinstein AA, Wijdicks EFM, et al. Spontaneous posterior spinal artery infarction: An under-recognized cause of acute myelopathy. *Neurology* 2018;91(9):414–417.
- Diehn FE, Maus TP, Morris JM, et al. Uncommon Manifestations of Intervertebral Disk Pathologic Conditions. *RadioGraphics* 2016;36(3): 801–823.
- Mulliken JB, Glowacki J. Hemangiomas and vascular malformations in infants and children: a classification based on endothelial characteristics. *Plast Reconstr Surg* 1982;69(3):412–422.
- Wang MX, Kamel S, Elsayes KM, et al. Vascular Anomaly Syndromes in the ISSVA Classification System: Imaging Findings and Role of Interventional Radiology in Management. *RadioGraphics* 2022;42(6):1598–1620.
- Takai K. Spinal Arteriovenous Shunts: Angioarchitecture and Historical Changes in Classification. *Neurol Med Chir (Tokyo)* 2017;57(7):356–365.
- DiChiro G, Doppman J, Ommaya, A. Radiology of Spinal Arteriovenous Malformations. In: *Progress in Neurological Surgery*, 1971.
- Heros RC, Debrun GM, Ojemann RG, Lasjaunias PL, Naessens PJ. Direct spinal arteriovenous fistula: a new type of spinal AVM. Case report. *J Neurosurg* 1986;64(1):134–139.
- Rodesch G, Hurth M, Alvarez H, Tadié M, Lasjaunias P. Classification of spinal cord arteriovenous shunts: proposal for a reappraisal—the Bicêtre experience with 155 consecutive patients treated between 1981 and 1999. *Neurosurgery* 2002;51(2):374–379; discussion 379–380.
- Strauss SB, Steinklein JM, Phillips CD, Shatzkes DR. Intraosseous Venous Malformations of the Head and Neck. *AJNR Am J Neuroradiol* 2022;43(8):1090–1098.
- Sharma R. Cerebral cavernous venous malformation. *Radioopaedia*. <https://radioopaedia.org/articles/cerebral-cavernous-venous-malformation?lang=us>. Published May 2008. Updated January 3, 2024. Accessed July 1, 2023.

36. Kuroedov D, Cunha B, Pamplona J, Castillo M, Ramalho J. Cerebral cavernous malformations: Typical and atypical imaging characteristics. *J Neuroimaging* 2023;33(2):202–217.
37. Koester SW, Scherschinski L, Srinivasan VM, et al. Radiation-induced cavernous malformations in the spine: patient series. *J Neurosurg Case Lessons* 2023;5(23):CASE22482.
38. Rastogi K, Klein CJ, O'Toole JE, Jhaveri MD, Malik R. Radiation-induced spinal nerve root cavernous malformations as a rare cause of radiculopathy. *Neurology* 2017;89(22):2299–2300.
39. Farid N, Zyroff J, Uchiyama CM, Thorson PK, Imbesi SG. Radiation-induced cavernous malformations of the cauda equina mimicking carcinomatous or infectious meningitis. A case report. *J Neuroimaging* 2014;24(1):92–94.
40. Ducray F, Guillemin R, Psimaras D, et al. Postradiation lumbosacral radiculopathy with spinal root cavernomas mimicking carcinomatous meningitis. *Neuro-oncol* 2008;10(6):1035–1039.
41. Sun I, Pamir MN. Spinal Cavernomas: Outcome of Surgically Treated 10 Patients. *Front Neurol* 2017;8:672.
42. Madhugiri VS, Ambekar S, Roopesh Kumar VR, Sasidharan GM, Nanda A. Spinal aneurysms: clinicoradiological features and management paradigms. *J Neurosurg Spine* 2013;19(1):34–48.
43. Alomari S, Xu R, Huang J, Tamargo R, Bydon A. Isolated aneurysms of the spinal circulation: a systematic review of the literature. *Neurosurg Rev* 2022;45(2):989–1008.
44. Renieri L, Raz E, Lanzino G, et al. Spinal artery aneurysms: clinical presentation, radiological findings and outcome. *J Neurointerv Surg* 2018;10(7):644–648.
45. Kranz PG, Amrhein TJ, Gray L. CSF Venous Fistulas in Spontaneous Intracranial Hypotension: Imaging Characteristics on Dynamic and CT Myelography. *AJR Am J Roentgenol* 2017;209(6):1360–1366.
46. Kranz PG, Gray L, Malinzak MD, Houk JL, Kim DK, Amrhein TJ. CSF-Venous Fistulas: Anatomy and Diagnostic Imaging. *AJR Am J Roentgenol* 2021;217(6):1418–1429.
47. Kranz PG, Gray L, Amrhein TJ. Decubitus CT Myelography for Detecting Subtle CSF Leaks in Spontaneous Intracranial Hypotension. *AJNR Am J Neuroradiol* 2019;40(4):754–756.
48. Schievink WI, Maya MM, Moser FG, et al. Lateral decubitus digital subtraction myelography to identify spinal CSF-venous fistulas in spontaneous intracranial hypotension. *J Neurosurg Spine* 2019;31(6):1–4.
49. Shatzkes DR. Vascular anomalies: Description, classification and nomenclature. <https://appliedradiology.com/articles/vascular-anomalies-description-classification-and-nomenclature>. Published September 22, 2018. Accessed July 1, 2023.
50. Chundriger Q, Tariq MU, Abdul-Ghafar J, Ahmed A, Din NU. Kaposiform Hemangioendothelioma: clinicopathological characteristics of 8 cases of a rare vascular tumor and review of literature. *Diagn Pathol* 2021;16(1):23.
51. Gottumukkala S, Srivastava U, Brocklehurst S, et al. Fundamentals of Radiation Oncology for Treatment of Vertebral Metastases. *RadioGraphics* 2021;41(7):2136–2156.
52. Premat K, Shotar E, Burns R, et al. Reliability and accuracy of time-reolved contrast-enhanced magnetic resonance angiography in hypervascular spinal metastases prior embolization. *Eur Radiol* 2021;31(7):4690–4699.
53. Na JH, Kim HS, Eoh W, Kim JH, Kim JS, Kim ES. Spinal cord hemangioblastoma : diagnosis and clinical outcome after surgical treatment. *J Korean Neurosurg Soc* 2007;42(6):436–440.
54. Waldron JS, Cha S. Radiographic features of intramedullary spinal cord tumors. *Neurosurg Clin N Am* 2006;17(1):13–19.
55. Baker KB, Moran CJ, Wippold FJ 2nd, et al. MR imaging of spinal hemangioblastoma. *AJR Am J Roentgenol* 2000;174(2):377–382.
56. Das A, Singh PK, Suri V, Sable MN, Sharma BS. Spinal hemangiopericytoma: an institutional experience and review of literature. *Eur Spine J* 2015;24(Suppl 4):S606–S613.
57. Louis DN, Perry A, Reifenberger G, et al. The 2016 World Health Organization Classification of Tumors of the Central Nervous System: a summary. *Acta Neuropathol (Berl)* 2016;131(6):803–820.
58. Singla R, Singh PK, Khanna G, et al. An institutional review of 10 cases of spinal hemangiopericytoma/solitary fibrous tumor. *Neurol India* 2020;68(2):448–453.
59. Rykkem JB, Diehn FE, Hunt CH, et al. Rim and flame signs: postgadolinium MRI findings specific for non-CNS intramedullary spinal cord metastases. *AJNR Am J Neuroradiol* 2013;34(4):908–915.
60. Langdon J, Way A, Heaton S, Bernard J, Molloy S. The management of spinal metastases from renal cell carcinoma. *Ann R Coll Surg Engl* 2009;91(8):649–652.
61. Manke C, Bretschneider T, Lenhart M, et al. Spinal metastases from renal cell carcinoma: effect of preoperative particle embolization on intraoperative blood loss. *AJNR Am J Neuroradiol* 2001;22(5):997–1003.